Transmission of a two-dimensional quantum point contact with the size varied from a single atom to a continuous wire; size effects

1995 J. Phys.: Condens. Matter 7 3597

(http://iopscience.iop.org/0953-8984/7/18/023)

J. Phys.: Condens. Matter 7 (1995) 3597–3613. Printed in the UK

Transmission of a two-dimensional quantum point contact with the size varied from a single atom to a continuous wire; size effects

Lyuba I Malysheva and Alexander I Onipko
Bogolyubov Institute for Theoretical Physics, Kiev 252143, Ukraine

Received 8 November 1994, in final form 13 February 1995

Abstract. The transmission through a two-dimensional (2D) channel, which connects semi-infinite 2D electron gas reservoirs and can be used as a model of both the few-atom-size (microscopic) and mesoscopic contact, is investigated under the assumption of the zero-field ballistic motion of electrons in the system. An analytical theory is advanced to a nearly exact analytical expression for the transmission probability verified by numerical calculations for a vast variety of channel parameters. On these bases a detailed analytical and numerical analysis of size effects in the quantum point contact (QPC) transmission is performed with emphases put on basic distinctions between atomic-size and mesoscopic-size QPC. The QPC properties are visualized in calculations of transmission against Fermi energy dependences for some representative channel parameters.

The results obtained are directly applicable to the description of coherent excitation energy transfer in relevant molecular 2D geometries. The suggested formalism can be also used for an analytical analysis of some other problems of current dispute, in particular, of non-linear field effects and 3D QPC properties.

1. Introduction

Since the effect of the zero-voltage, low-temperature DC conductance quantization was discovered in split-gate configurations of the two-dimensional electron gas (2DEG) [1, 2], theoretical description of the ballistic electron transport through a channel (constriction), which connects two 2DEG reservoirs, has become a classic problem addressed by many authors [3–19]. In the cited papers, the role of different factors (e.g. the size [4, 5, 13], geometry [5, 10, 13, 17], temperature [5, 13], impurities [11, 14], electric and magnetic fields [3, 6–9, 12, 15, 16, 18, 19]) in the conductance of the system often referred as a quantum point contact (QPC) has been investigated.

It is usually assumed that a QPC can be viewed as a section of a continuous wire defined in terms of a certain potential profile for electrons in the contact region. Such a model implies the mesoscopic size of the QPC, which is the case of the split-gate experiments. Another situation arises in the STM or QPC spectroscopy experimental arrangements, where the contact size is varied at the atomic level [20]. It is essential therefore, to study the manifestation of size effects up to the case of few-atom contacts. Obviously, the continuous-wire QPC model is not appropriate for this purpose.

One of the models which takes into account the discrete (atomic) structure of a real QPC is a 1s tight-binding model successfully used in a number of relevant studies of effects of impurities and wire width variation [21], geometry [22, 23], magnetic field [24, 25],

0953-8984/95/183597+17$19.50

etc. Here, this model is used for description of transmission properties of wide–narrow–wide (WNW) geometry with emphases put on distinctions in properties of atomic-size and mesoscopic-size contacts.

Due to Landauer's original work [26] electrical QPC conductance can be related to the transmission probability through a QPC between two temperature baths. Subsequently developed formalism (see [27–29] for references) has been successfully used in a great number of studies of the QPC transmission and conductance performed mostly by numerical methods. Only in very a few cases of not particularly realistic adiabatic potentials experienced by electrons in the QPC region can the transmission coefficient be found analytically. In general, this is a computational task because the transmission is essentially a multimode process. The case of strongly non-adiabatic WNW structure considered here is not an exception in this sense and much computational effort has been spent on its precise description, see for example [4, 13]. Nevertheless, we have succeeded in the formulation of an analytical theory for the QPC transmission which being used for quantitative analysis has proven to be exact within few per cent. The derivation of corresponding relations and their application to description of size effects throw, as we believe, some extra light upon QPC properties. In particular, the model used enables us to reveal basic distinctions and similarities between size effects in atomic-size and mesoscopic-size contacts and their dependence on QPC parameters.

The QPC model is specified in section 2. Section 3 briefly summarizes the calculation method which yields an analytical expression for the transmission coefficient for both discrete and continuous models of the WNW structure. To make transparent the underlying physics and to simplify comparison with previous results, this expression is rederived in an equivalent form in appendix B, where WNW structure is treated as two wide–narrow (WN) structures connected in series. In section 4, the derived relations are used for quantitative description of gross and fine (resonance) structure of the QPC transmission spectrum. Some results of numerical calculations are also presented to facilitate understanding of specific properties of atomic-size contacts. Appendix A contains some relations for reference.

2. Model statement

The discrete QPC model is specified in figure 1. This is a hard-wall wide–narrow–wide configuration, which is shown by a solid line and supposed to be built up of one-level atoms coupled by the electron resonant transfer interaction L between the nearest neighbours. Outside the structure the electron energy is infinite, and at the lattice sites it is set equal to zero. Then, in terms of the Fermi operators of the creation (a_r^+) and annihilation (a_r) of an electron at the lattice site with the coordinates $r = (m, n)$, the heterostructure Hamiltonian takes the form

$$\hat{H} = L \sum_{|r-r'|=a} a_r^+ a_{r'}$$

where a is the lattice constant, and the choice of the site numbering along the m- and n-axis is shown in figure 1.

In the next section we obtain the formal definition for the transmission coefficient, which is valid for an arbitrary width of wide and narrow parts of the structure denoted by $\mathcal{N}$ and N, respectively. But the main attention is paid here to the case $\mathcal{N} \to \infty$. Semi-infinite parts of the latter structure associate with the source and drain electron reservoirs characterized by a conductance band width of $8|L|$ which is symmetric with respect to the zero electron energy. Such a QPC model, see figure 2(a), is attractive at least in two aspects. On one

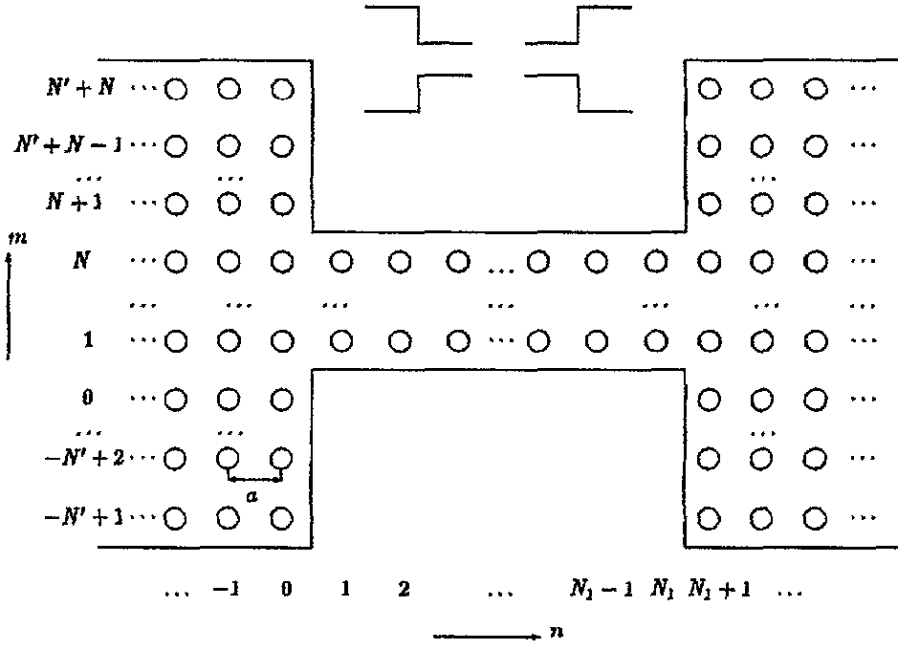

Figure 1. Wide–narrow–wide (WNW) geometry formed by a regular square lattice with the lattice constant a. The width of the wide and narrow parts of the structure expressed in the lattice site number is denoted by $\mathcal{N}$ and N, respectively; $N' = \frac{1}{2}(\mathcal{N} - N)$; the length of the channel between the wide parts (reservoirs) is N_1. Each lattice site is assumed to be occupied by a one-level atom coupled with the nearest neighbours via the electron resonant transfer interaction L. In the continuum limit, $N \to \infty$, $Na =$ constant, the model is equivalent to a WNW structure (shown by solid line) with the parameters $(\mathcal{N} + 1)a$—reservoir width, $w = (N + 1)a$—channel width, $l = (N_1 - 1)a$—channel length. The WNW structure can be regarded as a compound device—a connection of two wide–narrow (WN) structures shown in the inset.

hand, it enables one to pass to the continuum limit, $N \to \infty$, $aN =$ constant and, thereby, to the continuous-wire model of the QPC exploited by many authors in previous studies of the QPC conductance properties (references [3–19] are given to name few). The electron dynamics in this case is determined by the effective mass $m^* = \hbar^2/2La^2$. So, the model at hand does not pretend to reproduce correctly the full band shape of relevant semiconductor heterostructures, but it does reproduce the bottom of the conductance band provided that the constant-effective-mass approximation works and under the appropriate choice of the L value. On the other hand, when N is finite, see figure 2(b)–(d), one deals with a finite-number-of-states contact between two conductors characterized by the infinite number of electron states (the typical situation in STM experiments). Thus, a unique possibility is presented to trace how an atom-size contact acquires properties of a continuous-wire contact.

3. Calculation method

3.1. General relations

In the framework of the Landauer–Büttiker approach to the problem of the QPC conductance, see [27–29] and references therein, the main quantity to be calculated is the total through

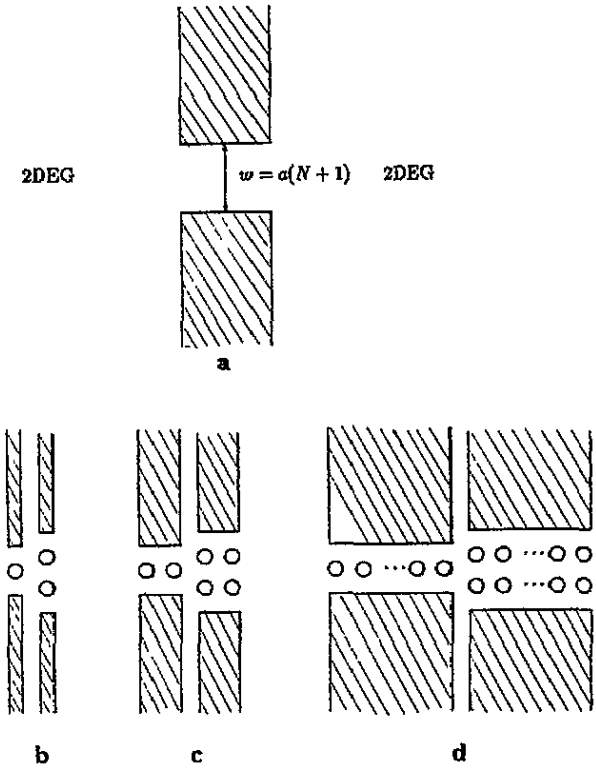

Figure 2. Model of the quantum point contact (QPC) between two semi-infinite 2DEG reservoirs used in this paper (a) and its particular realizations: one- and two-atom width contacts one (b), two (c), and arbitrary (d) number of atoms in length. Regions inaccessible for electrons are shaded. The zero-field transmission of contacts (b)–(d) is exactly described by equation (7).

channel transmission coefficient. By definition, it is

$$T_{\mathrm{WNW}}(E, V) = \sum_{j_s=1}^{\bar{j}_s} \sum_{j_d=1}^{\bar{j}_d} \frac{\sin k'_{j_d}}{\sin k_{j_s}} |t_{k'_{j_d} k_{j_s}}|^2 \tag{1}$$

where k_{j_s} and k'_{j_d} are the wave vectors of incident and transmitted electrons, $\bar{j}_{s(d)}$ denotes the highest propagating mode in the source (drain) reservoir, and $t_{k'_{j_d} k_{j_s}}$ the transmitted wave amplitudes, which are to be found from the stationary Schrödinger equation with scattering-type boundary conditions.

For the model at hand, instead of solving the corresponding set of equations, which connect $t_{k'_{j_d} k_{j_s}}$ with the amplitudes of the incident (given) and reflected waves, it is more convenient to operate with the electron wave function inside the channel, precisely, with its jth-mode amplitudes on the entrance ($n = 1$) and exit ($n = N_1$) sites of the channel. Denoting the appropriate quantities by X_1^j and $X_{N_1}^j$, and omitting lengthy but elementary intermediate calculations, we write only the resulting equations in the form

$$\left(\tilde{G}^j_{N_1,N_1} + \cos\frac{\pi j}{N+1} - E\right) X_1^j - \tilde{G}^j_{N_1,1} X_{N_1}^j = 1 + \mathrm{i} \sum_{j'=1}^{N} \frac{v_{j_s j'}}{v_{j_s j}} A_{jj'} X_1^{j'} \tag{2}$$

$$-\tilde{G}^{j}_{N_1 1}X^{j}_{1}+\left(\tilde{G}^{j}_{11}+eV+\cos\frac{\pi j}{N+1}-E\right)X^{j}_{N_1}=\mathrm{i}\sum_{j'=1}^{N}\frac{\nu_{j_s j'}}{\nu_{j_s j}}A'_{jj'}X^{j'}_{N_1}. \quad (3)$$

Here, E is the electron energy (in units $2L$), eV is the difference in the site energies between the entrance and exit of the channel, which arises due to the voltage drop V. The quantities

$$\nu_{j_s j}=\sum_{m=1}^{N}\sin\left(\frac{\pi j_s(m+N')}{\mathcal{N}+1}\right)\sin\left(\frac{\pi jm}{N+1}\right)$$

and

$$A_{jj'}(E)=\frac{4}{(\mathcal{N}+1)(N+1)}\sum_{j_s=1}^{\mathcal{N}}\sin k_{j_s}\nu_{j_s j}\nu_{j_s j'}$$
$$\equiv\Re(A_{jj'})+\mathrm{i}\Im(A_{jj'}) \qquad (A'_{jj'}(E)=A_{jj'}(E-eV))$$

appear in (2), (3) because of the non-orthogonality of source (drain) and channel basis wave functions which describe the transverse electron motion. Equations (2) and (3) also include one-dimensional Green functions in combinations

$$\tilde{G}^{j}_{n,n'}(E,V)=\frac{G^{j}_{n,n'}(E,V)}{G^{j}_{1,1}(E,V)G^{j}_{N_1,N_1}(E,V)-\left(G^{j}_{N_1,1}(E,V)\right)^2} \quad (4)$$

where the matrix elements $G^{j}_{n,n'}(E,V)$ obey the equation

$$2\left(E-\cos\frac{\pi j}{N+1}-\frac{n-1}{N_1-1}eV\right)G^{j}_{n,n'}-(1-\delta_{n,1})G^{j}_{n-1,n'}-(1-\delta_{n,N_1})G^{j}_{n+1,n'}=\delta_{n,n'} \quad (5)$$

written under assumption of linear voltage drop along the channel.

In terms of solutions to the set (2), (3), the definition (1) can be rewritten as

$$T_{\mathrm{WNW}}(E,V)=4\sum_{j,j'=1}^{N}\Re(A_{jj'})\Re(A'_{jj'})X^{j}_{N_1}X^{j'*}_{N_1}. \quad (6)$$

Equations (2)–(6) determine (in the channel wave functions basis) the through channel transmission as a function of electron energy, the bias, channel parameters, and the width of wide parts of the WNW structure. As is shown below, the calculation scheme presented is to some extent similar to that used by Szafer and Stone [5] but has wider applications. In particular, it is equally applicable to the description of QPC properties at the atomic and mesoscopic levels; it includes the case of biased channels; and finally, despite finding T is, in general, a computational problem, the derived equations suggest an analytical expression for the transmission coefficient proved to be remarkably accurate. The latter is the most significant advantage of the present approach in comparison with numerous computational studies of similar QPC models.

3.2. Diagonal approximation

In what follows, we restrict ourselves to consideration the case of infinitely large reservoir width, (i.e., to the QPC models shown in figure 2) and zero bias $eV=0$. The zero-field transmission coefficient taken at the Fermi energy E_F determines the linear-response zero-temperature QPC conductance [27–29].

Using explicit expressions for matrix elements $A_{jj'}$ (see appendix A), it is easy to show that $A_{jj} \ll A_{jj'}$ for $E_j^o \leqslant E_F = 2 - E \leqslant E_{j+1}^o$, where E_j^o stands for the opening energy of the jth-channel mode. This property (first noted by Szafer and Stone [5]) justifies the approximation $A_{jj'} = \delta_{jj'} A_{jj}$ in (2), (3), and (6) and straightforwardly leads to the following expression for the transmission coefficient

$$T_{WNW}(E,0) = \sum_{j=1}^{N} T_{WNW}^{j}$$

$$= 4\sum_{j=1}^{N} \frac{\left(\Re(A_{jj})\tilde{G}_{N_1,1}^{j}\right)^2}{\left|\left[\tilde{G}_{1,1}^{j} + \cos[\pi j/(N+1)] - E - iA_{jj}\right]^2 - \left[\tilde{G}_{N_1,1}^{j}\right]^2\right|^2} \tag{7}$$

where A_{jj} and tilded Green functions for an unbiased channel are defined in equations (A2), (A3) and (A5), respectively.

Note that for one- and two-atom width channels (see models (b)–(d) in figure 2) definition (7) is exact. In the case of arbitrary N, deviations in the energy dependence (7) from the exact values of T_{WNW} do not exceed a few per cent. This was verified by comparison of (7) with exact calculations for a vast variety of channel parameters.

It is worth emphasizing that we deal here with an extreme case of a 'non-adiabatic' QPC model, where mixing of channel and reservoir modes (*a priori* absent in adiabatic models) is strong. This mode-mixing effect, which results in electron wave reflection from channel ends and gives rise to the resonance structure of the transmission spectrum (discussed below), is mainly included by passing from (1) to the transmission description in the channel wave function basis (7). Therefore (and because of the weakness of channel mode mixing), it is not surprising that T_{WNW} determined in the diagonal approximation gives a practically exact description of essentially multireservoir mode transmission.

To bridge the present and previous results, most of which have been obtained for the continuous QPC model, it is helpful to rewrite (7) in the effective mass approximation. For this, we set $L = -\hbar^2/(2m^*a^2)$, where the electron effective mass m^* is positive. It is also convenient to introduce the quantity $ak_{th} = \pi/(N+1)$ which has the meaning of the propagation threshold wave vector in a channel of the width $w = (N+1)a$, and to use the propagation threshold energy $\varepsilon_{th} = \hbar^2\pi^2/(2m^*w^2)$ as the energy unites. Using these notations in equation (7), which is taken in the limit $N \to \infty$, Na = constant, we get

$$\lim_{ak_{th}\to 0} T_{WNW}(E_F) = T_{WNW}^{c}(\varepsilon_F)$$

$$= \sum_{j=1}^{\infty} \frac{4q_j^2\Re^2(A_{jj}^c)/\sin^2(\pi q_j l/w)}{\left|\left(q_j\cot(\pi q_j l/w) - iA_{jj}^c\right)^2 - q_j^2/\sin^2(\pi q_j l/w)\right|^2} \tag{8}$$

where $\varepsilon_F = 2E_F/(a^2k_{th}^2) = q_j^2 + j^2$ denotes the dimensionless energy in units ε_{th} (as distinct from E_F measured here in $2|L|$), $l = (N_1 - 1)a$ is the length of the channel, and A_{jj}^c denotes an analogue of the matrix element A_{jj} in the continuum limit, $A_{jj}^c = \delta_{jj'}\lim_{ak_{th}\to 0}(ak_{th})^{-1}A_{jj'}$, see (A4).

The above equation is similar but not identical to the definition of T_{WNW}^{c} obtained by Szafer and Stone [5]. This similarity becomes obvious for an equivalent representation of (8) in terms of characteristics of the WN structure shown in figure 1, namely, the jth-mode transmission and reflection coefficients T_{WN}^{j} and R_{WN}^{j}, and the phase shift acquired by the jth-mode wave reflected from the WN discontinuity. The derivation of corresponding

expressions, which bring to light the physics underlying the jth-mode WNW transmission T^j_{WNW}, is given in appendix B.

4. Results and discussion

4.1. Gross structure of the transmission spectrum

Here, we have a look at the WNW structure as a compound system, see figure 1: two WN structures connected by a wire segment (characteristics of the WN structure which enter the definition of T^j_{WNW} are discussed in appendix B). In figure 3, the energy dependence $T^j_{\mathrm{WNW}}(E_{\mathrm{F}})$ is shown for $j = 1, 2, 3, 4, 5$ ($N = 5$, $\mathcal{N} = \infty$): curves (a) correspond to $N_1 = 1$, and (b) to $N_1 = 7$. The observations summarized below are independent of the choice of the parameters N and N_1.

First we note that as seen from the symmetry relations (B8) the partial jth-mode transmission possesses the following property: $T^j_{\mathrm{WNW}}(E < 0) = T^{N+1-j}_{\mathrm{WNW}}(|E|)$, which provides the parity of the total transmission. Therefore, similarly to $T_{\mathrm{WNW}}(E_{\mathrm{F}})$ we can restrict the presentation of the energy dependence of T^j_{WNW} to the interval $E_{\mathrm{F}} \in [0, 2]$.

In accordance with (B7), $T^j_{\mathrm{WN}} = 0$ at the energy of the jth-mode opening E°_j. However, at this point $T^j_{\mathrm{WNW}}(E^{\circ}_j) \neq 0$. For the given N, $T^j_{\mathrm{WNW}}(E^{\circ}_j)$ has the maximum value in the channel with $N_1 = 1$, $T^j_{\mathrm{WNW}} = \Re^2(A_{jj})/\,|A_{jj}|^2\big|_{E_{\mathrm{F}}=E^{\circ}_j}$. This value decreases very rapidly with the increase of the parameter $(N_1 - 1)/(N + 1)$ because of the suppression of the through channel tunnelling with the increase of the length-to-width ratio.

Above E°_j, T^j_{WNW} is close to unity in most of the jth-mode energy interval, where

$$\frac{(1 - R^j_{\mathrm{WN}})^2}{(1 + R^j_{\mathrm{WN}})^2} \equiv T^{j(\min)}_{\mathrm{WNW}} \leqslant T^j_{\mathrm{WNW}} \leqslant 1. \tag{9}$$

This is true even in the shortest possible channel, $N_1 = 1$, see figure 3(a). Note that due to the suppression of tunnelling and the interference effects, the increase of T^j_{WNW} is steeper in channels with larger length-to-width ratio (compare curves (a) and (b) in figure 3). The latter parameter also determines the resonance structure seen in figure 3b. When this structure appears, $T^{j(\min)}_{\mathrm{WNW}}$ plays the role of an enveloping function which describes the energy dependence of the transmission minima within the jth plateau.

For energies below E°_j, where $T^j_{\mathrm{WN}} + R^j_{\mathrm{NW}} \neq 1$, only the evanescent modes contribute to T^j_{WNW}. This contribution is suppressed very rapidly with the decrease of the electron energy. When E_{F} approaches E°_{j-1}, $T^j_{\mathrm{WNW}}(E_{\mathrm{F}})$ becomes nearly zero, because T^j_{WN} goes to zero, see appendix B.

Thus, due to the specific energy dependence of the partial transmission T^j_{WNW}, which, in due course, is determined by transport characteristics of the WN structure, the energy dependence of the total zero-field transmission coefficient T_{WNW} is very accurately reproduced by the following simple formula

$$T_{\mathrm{WNW}}(E_{\mathrm{F}} \in [E^{\circ}_j, E^{\circ}_{j+1}]) = j - 1 + T^j_{\mathrm{WNW}} + T^{j+1}_{\mathrm{WNW}}. \tag{10}$$

Since j is arbitrary, equation (10) completely determines the dependence $T_{\mathrm{WNW}}(E_{\mathrm{F}})$. If applied to the extended channels, $(N_1 - 1)/(N + 1) \geqslant 1$, the last term in this equation can be omitted. In the latter case, the structure of the formula for T_{WNW} is similar to (B12) for T_{WN}.

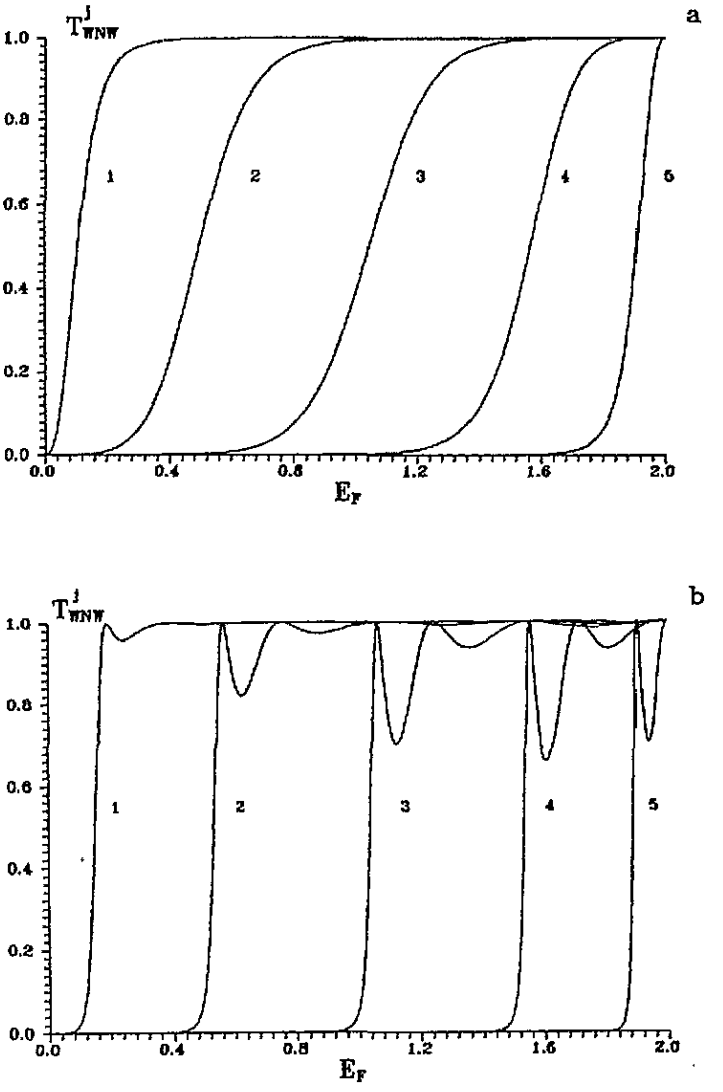

Figure 3. The jth-mode partial transmissions T^j_{WNW} as a function of the Fermi energy $E_F = 2 - E/2|L|$ in units $2|L|$ calculated for the five-atom width channel (j = 1–5) with $N_1 = 1$ (a) and 7 (b) atoms in length.

4.2. Fine resonance structure

As it was demonstrated by calculations of Kirczenow [4], Szafer and Stone [5], and other authors, the model under consideration predicts the appearance of resonances in the through QPC transmission dependence on the electron energy. So far, the resonance structure of the QPC transmission spectrum has been discussed on computational or phenomenological grounds. However, the main regularities of this structure can be easily explained using the analytical expression for the transmission coefficient (B6) (discrete model) or (B9) (continuous one) obtained in appendix B. Since the resonance structure is described in a

similar manner for both models in focus, we consider only the case of the continuous channel.

As mentioned above, the resonance structure of $T^{c}_{WNW}(\varepsilon_F)$ originates from the interference of electron waves reflected from the channel edges. According to equations (10), (B9), the position and the number of resonances in the jth plateau of the dependence of T^{c}_{WNW} on Fermi energy is determined by the solutions $q_j^{(n)}$, $n = 0, 1, 2, \ldots$, to the equation

$$\frac{l}{w}q_j + \pi^{-1}\phi^{c}_j(q_j) = n \qquad n = 0, 1, 2, \ldots \tag{11}$$

in the energy interval $j^2 \leqslant \varepsilon_F \leqslant (j+1)^2$, i.e. for $q_j \in [0, q_j^{c(max)}]$, $q_j^{c(max)} = \sqrt{2j+1}$. The left-hand side of (11) represents the change in the phase of the Fermi electrons with the de Broglie wavelength $\lambda^j_B = 2\pi(q_j k_{th})^{-1}$: the first term corresponds to the phase acquired as a result of the electron wave propagation at the distance l; the second is due to a single reflection from the channel edge. Just the latter term, which accounts for the reflection 'non-elasticity', makes (11) different from the standard condition of the interference resonances $n\lambda^j_B/2 = l$.

The phase ϕ^c_j defined in (B10) as a function of $q_j/q_j^{c(max)}$ varies very little with j. In particular, $\phi^c_j(q_j^{c(max)}) \approx -\pi/2$. Thus, the critical (minimal) length-to-width ratio of the channel, at which the first resonance appears in the jth plateau of the dependence $T^{c}_{WNW}(\varepsilon_F)$, can be written as

$$\left(\frac{l}{w}\right)_{cr}\sqrt{2j+1} = \pi^{-1}\left|\phi^{c}_j\left(\sqrt{2j+1}\right)\right| \approx \tfrac{1}{2} \tag{12}$$

and the total number of resonances within the jth plateau as

$$n^c_j = \left[\frac{l}{w}\sqrt{2j+1} + \pi^{-1}\phi^c_j(\sqrt{2j+1}) + 1\right] \approx \left[\frac{l}{w}\sqrt{2j+1} + \frac{1}{2}\right]. \tag{13}$$

The strength of the interference resonances described by (11)–(13) depends on their position. In the other words, not all n^c_j resonances in the jth plateau predicted by (11) will be observed equally well. The explanation of this effect is as follows. As seen from (B9), for all resonances within the jth plateau, the transmission coefficient has the same maximal value. By contrast, the values of T^{cj}_{WNW} at minima depend on the minimum position. This dependence (and thus the resonance strength) is completely determined by the enveloping function $T^{cj(min)}_{WNW} = (1 - R^{cj}_{WN})^2/(1 + R^{cj}_{WN})^2$ similar to that introduced in (9). Evidently, the decrease of the resonance strength follows the dependence $1 - T^{cj(min)}_{WNW} = 4R^{cj}_{WN}/(1 + R^{cj}_{WN})^2$ on $\Delta^c = \sqrt{\varepsilon_F} - j \in [0, 1]$. Since the jth-mode wave reflection in the channel falls nearly to zero (roughly speaking, halfway towards the next mode opening), the resonance peaks are also observed only in the first half of plateaus. Therefore, there is no one-to-one correspondence between the number of peaks really observed in the jth the plateau of the dependence $T^{c}_{WNW}(\sqrt{\varepsilon_F})$ and the total number of resonances n^c_j determined by equation (13).

4.3. Numerical results

Here, we present the results of exact calculations for the zero-field through QPC transmission coefficient to provide a visual quantitative picture of the size effects on the transmission of a 2D channel which connects two semi-infinite 2DEG reservoirs.

In figure 4(a) and 4(b) we grouped dependences $T_{WNW}(E_F)$ with the fixed length-to-width ratio $(N_1 - 1)/(N+1) = 1$ and 3, respectively. Each ratio value is represented by three curves with the different width and length of the channel. The length $N_1 - 1 = 6$, 12, 18

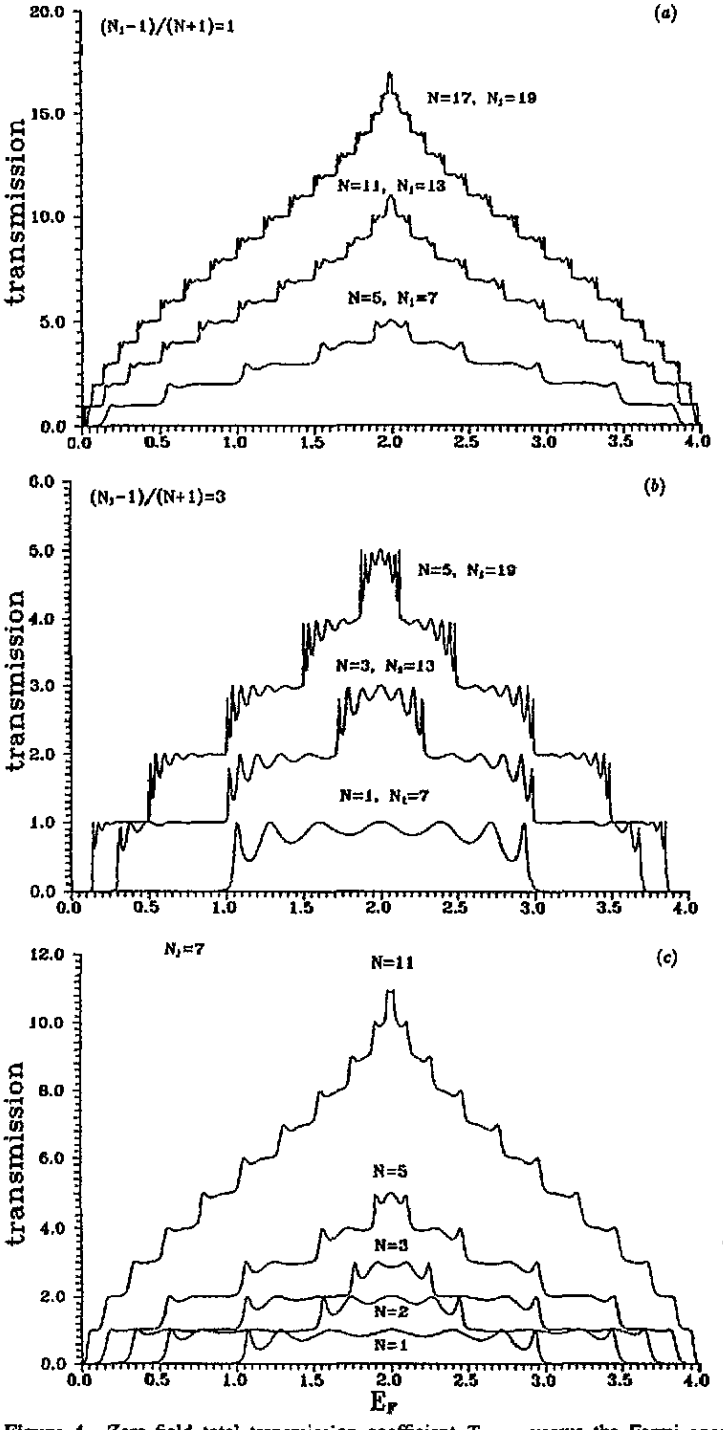

Figure 4. Zero-field total transmission coefficient T_{WNW} versus the Fermi energy. Curves (a), (b), correspond to constant values of the length-to-width ratio $(N_1 - 1)/(N + 1) = 1, 3$, respectively. Curves (c) to constant values of the channel length $N_1 = 7$. Each curve in groups (a), (b) is labelled by values of the channel length (N_1) and width (N), and in group (c) by values of N. Curves (d) represent $T_{WNW}(\sqrt{E_F/E_1^0})$ for $N_1 = 19$, $N = 5, 11, 35$ shown by solid lines, and $T^c_{WNW}(\sqrt{\varepsilon_F})$ for $l/w = 3, 1.5, 0.5$ (upper, middle, and lower curves, respectively) by dashed lines.

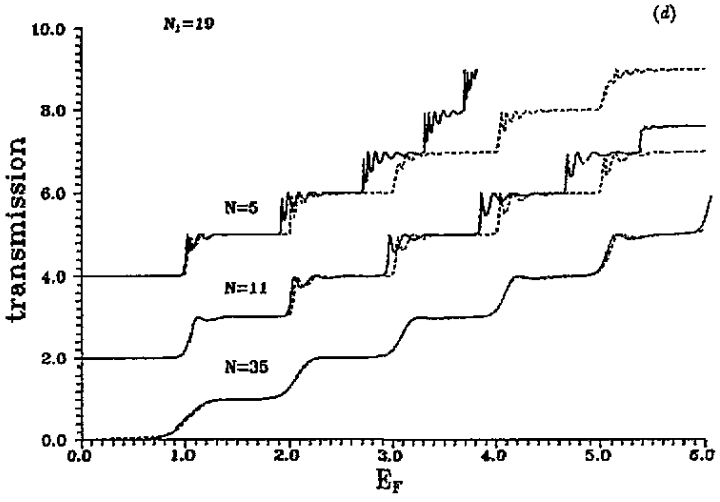

Figure 4. Continued

appears in both groups, to make apparent the transmission dependence on the channel width at the fixed length. This same dependence is illustrated in figure 4(c), by the presentation of five curves calculated for $N_l = 7$, and $N + 1 = 2, 3, 4, 6$, and 12. Thus, curves (a)–(c) in figure 4 display the most characteristic size effects predicted by the discrete QPC model. For comparison with its continuous analogue, the QPC transmission for $N_l = 19$ and $N = 5$, 11, and 35 is plotted in figure 4(d) versus $\sqrt{E_F/E_{th}}$ ($\rightarrow \sqrt{\varepsilon_F}$ in the continuum limit) together with the corresponding dependences $T^c_{WNW}(\varepsilon_F)$. The latter illustration makes visible how a contact built of atoms acquires properties of a continuous-wire contact. Curves of figure 4 are used below in discussion of basic distinctions between the discrete and continuous QPC models.

In accordance with its definition, the transmission of the discrete channel is always restricted in magnitude. This limitation is due to the finite number of states available for electrons arriving from the source (drain) reservoir to the channel entrance (exit). In the given model of one-level atoms, the maximal value of the total transmission coefficient equals the channel width in the number of atoms. The maximal transmission is attained when all states of the transverse quantization in the channel are occupied, i.e., when the electron energy is in the vicinity of the middle of the conductance band. With the further increase of E_F, the propagating modes close one by one. The decrease in the number of channel states available for electrons results in descending staircases which represent T_{WNW} against E_F dependences shown in figure 4(a)–4(c). The overall tendency in the transmission to decrease for energies $E_F > 2$ is caused by the decrease of the electron group velocity, when the electron energy goes to the top of the conductance band. In this sense, the existence of the maximum in the gross structure of the transmission dependence versus the Fermi energy represents a general QPC property, if one takes into account the finiteness of the conductance band width.

As is known, in the continuous model, the transmission depends only on ε_F—the Fermi energy—in units of ε_F and the length-to-width ratio in the channel. It means that for l/w = constant, T^c_{WNW} varies identically with changes of the Fermi energy at the fixed channel width and, *vice versa*, with changes of w at fixed $\varepsilon_F\varepsilon_{th}$. As a result, an integer-fold increase in w is responded, to within an accuracy of unity, by the same increase in T^c_{WNW},

see figure 4(d). In other words, the continuous channel transmission with the same accuracy obeys the law $T^c_{WNW}(w)/T^c_{WNW}(w') = w/w'$. By contrast, curves in figure 4(b) show that contacts of few atoms in width are quite far from following the regularity just mentioned. Let us compare, for example, curves $N = 1$, $N_1 = 7$ with $N = 3$, $N_1 = 13$ (twofold increase in $N + 1$) and with $N = 5$, $N_1 = 19$ (threefold increase in $N + 1$). It is seen that the twofold and threetimes increase in the width may result in twofold, threefold, and threefold to five-times increase in the transmission, respectively (again, we refer here to the idealized square-corner-shaped plateaus in the transmission, i.e. the resonance structure is not taken into account).

Probably the most striking result is that some plateaus in transmission against Fermi energy dependences, which describe channels of different width, are overlapped. As seen from figure 4(d), there exists an energy interval, where the transmission coefficient for contacts with three, four (not shown), and five atoms in width is the same (disregarding the resonance structure of the plateaus). This result is in sharp contradiction with predictions of the continuous model. However, for high-lying plateaus (but well below the middle of the conductance band) the difference between $T_{WNW}(N)/T_{WNW}(N')$ and $T^c_{WNW}(w)/T^c_{WNW}(w')$ is small for N, $N' > 10$ and diminishes very rapidly with the increase of j.

5. Conclusion

Two equivalent analytical expressions for the transmission probability through a rectangular constriction in a 2DEG are derived. One (presented in section 2) is based on the Green function method and thus, it is flexible for adjusting to more complex QPC models. The other (described in appendix B) is obtained by using an original version of the transfer matrix method [30]. The latter has proven to be transparent physically and was used therefore for quantitative analytical analysis of the QPC transmission spectrum. Another reason for its inclusion is that a similar, but not equivalent, definition of T^c_{WNW} as given in (B9), has been derived by Szafer and Stone [5] but, unfortunately, the corresponding expression is presented in the original paper with misleading misprints.

The above-derived relations give a precise description of the QPC transmission spectrum, which is much better than that given by the mean-field approximation suggested in [5]. In particular, they predict the number and position of resonances which in previous works could be unambiguously determined only in rather lengthy computations.

Thus, the suggested method is highly efficient for quick and reliable analysis of size effects in transmission (and conductance) of non-adiabatic contacts. Some nearest perspectives of its applications are worth mentioning.

It is straightforwardly applicable to analysis of high-field non-linear effects modelled by biased electron potential energy inside the contact and (or) the presence of the potential difference between the contact ends. Standard methods (say, matching technique) demand using supercomputers in this case and are inefficient for studying fine effects such as additional conductance quantization recently observed in high fields [31].

The generalization of the present method to the case of the 3D system will give a tractable model of atomic-size contacts realized in STM experiments.

Finally, this method can be directly used for the description of coherent excitation energy transfer effects in molecular layers with the given and other restricted geometries, which can serve as prototypes of optoelectronic devices.

Acknowledgment

This research was partly supported by grant No INTAS-93-85.

Appendix A

Here, we present for reference explicit expressions for matrix elements $A_{jj'}$ in the case of $\mathcal{N} = \infty$ and tilded Green functions $\tilde{G}_{1,1}$ and $\tilde{G}_{1,N_1}$ in an unbiased channel, which complete the definition of the transmission coefficient given in equation (7).

By passing in

$$\begin{aligned} \Re(A_{jj'}(E)) &= \frac{4}{(\mathcal{N}+1)(N+1)} \sum_{j_s=1}^{\bar{j}_s} \sin k_{j_s} v_{j_s j} v_{j_s j'} \\ \Im\left(A_{jj'}(E)\right) &= \frac{4}{(\mathcal{N}+1)(N+1)} \sum_{j_s=\bar{j}_s+1}^{N} \sinh k_{j_s} v_{j_s j} v_{j_s j'} \end{aligned} \tag{A1}$$

from the summation over reservoir modes to integration, one easily gets

$$\begin{aligned} \Re(A_{jj'}) = {} & \frac{2\sin(\pi j/(N+1))\sin(\pi j'/(N+1))}{\pi(N+1)} \\ & \times \int_0^{\bar{x}} \mathrm{d}x \frac{\sqrt{1-(E/2L-\cos x)^2}}{(\cos x - \cos[\pi j/(N+1)])(\cos x - \cos[\pi j'/(N+1)])} \begin{cases} \sin^2([(N+1)/2]x) & \text{even } j, j' \\ \cos^2([(N+1)/2]x) & \text{odd } j, j' \end{cases} \\ \Im(A_{jj'}) = {} & \frac{2\sin(\pi j/(N+1))\sin(\pi j'/(N+1))}{\pi(N+1)} \\ & \times \int_{\bar{x}}^{\pi} \mathrm{d}x \frac{\sqrt{(E/2L-\cos x)^2-1}}{(\cos x - \cos[\pi j/(N+1)])(\cos x - \cos[\pi j'/(N+1)])} \begin{cases} \sin^2([(N+1)/2]x) & \text{even } j, j' \\ \cos^2([(N+1)/2]x) & \text{odd } j, j' \end{cases} \end{aligned} \tag{A2}$$

where $\bar{x} = \cos^{-1}(E/2L - 1)$, $E \geqslant 0$. For $E < 0$

$$A_{jj'}(E<0) = A^*_{N+1-j\,N+1-j'}(|E|). \tag{A3}$$

In the continuum limit, the corresponding matrix elements $A^c_{jj'} = \lim_{ak_{th}\to 0}(ak_{th})^{-1}A_{jj'}$ $\equiv \Re(A^c_{jj'}) + \mathrm{i}\Im(A^c_{jj'})$ take the form

$$\begin{aligned} \Re(A^c_{jj'}) &= \frac{8}{\pi^2} jj' \int_0^{\sqrt{\varepsilon_F}} \mathrm{d}x \frac{\sqrt{\varepsilon_F - x^2}}{(j^2-x^2)(j'^2-x^2)} \begin{cases} \sin^2((\pi/2)x) & \text{even } j, j' \\ \cos^2((\pi/2)x) & \text{odd } j, j' \end{cases} \\ \Im(A^c_{jj'}) &= \frac{8}{\pi^2} jj' \int_0^{1/\sqrt{\varepsilon_F}} \mathrm{d}x \frac{x\sqrt{1-\varepsilon_F x^2}}{(j^2x^2-1)(j'^2x^2-1)} \begin{cases} \sin^2(\pi/2x) & \text{even } j, j' \\ \cos^2(\pi/2x) & \text{odd } j, j'. \end{cases} \end{aligned} \tag{A4}$$

The solution of equation (5) for $V = 0$ gives

$$\begin{aligned}
&\tilde{G}^{0j}_{1,1} = \tilde{G}^{0j}_{N_1,N_1} = \frac{\sin(N_1 k_j)}{\sin((N_1-1)k_j)} \qquad \tilde{G}^{0j}_{1,N_1} = \frac{\sin k_j}{\sin((N_1-1)k_j)} \\
&\tilde{G}^{0j}_{1,1}(E<0) = \tilde{G}^{0j}_{N_1,N_1}(E<0) = -\tilde{G}^{0\,N+1-j}_{1,1}(|E|) \\
&\tilde{G}^{0j}_{1,N_1}(E<0) = (-1)^{N_1}\tilde{G}^{0\,N+1-j}_{1,N_1}(|E|)
\end{aligned} \tag{A5}$$

where k_j is defined by the equation $\cos k_j = E/2L - \cos[\pi j/(N+1)]$.

Appendix B

In terms of solutions of the scattering problem for a wide–narrow structure, the total zero-field transmission coefficient for a constriction as shown in figure 1 takes the form [31]

$$T_{\mathrm{WNW}} = \sum_{j=1}^{N} T^{j}_{\mathrm{WNW}} \tag{B1}$$

where (compare with (6))

$$T^{j}_{\mathrm{WNW}} = \sum_{j_2=1}^{N}\left|\sum_{j_1=1}^{N}\sum_{j_s=1}^{\bar{j}_s}\left(\frac{\hat{p}}{\hat{I}-(\hat{p}\hat{r}^{\mathrm{WN}})^2}\right)_{jj_1}\hat{t}^{\mathrm{WN}}_{j_1 j_s}\left(\hat{t}^{\mathrm{WN}}_{j_2 j_s}\right)^{*}\right|^2. \tag{B2}$$

In (B1), (B2), the indices j, j_1, j_2 refer to the modes of the narrow part, whereas j_s refers to the wide part of the WN structure, respectively; $\hat{p}$ is the diagonal operator with the matrix elements $\hat{p}_{jj'} = \delta_{jj'}\exp[ik_j(N_1-1)]$; the matrix element $\hat{r}^{\mathrm{WN}}_{jj'} = \sqrt{(\sin k_j/\sin k_{j'})}r^{\mathrm{WN}}_{jj'}$ of the operator $\hat{r}^{\mathrm{WN}}$ is the probability amplitude of the j'th-to-jth-mode reflection in the narrow part of the structure, and $\hat{t}^{\mathrm{WN}}_{jj_s} = \sqrt{(\sin k_j/\sin k_{j_s})}t^{\mathrm{WN}}_{jj_s}$ represents the probability amplitude of the transmission into the jth-mode wave in the narrow part of the WN structure from the j_sth-mode wave in the wide part.

The quantities $t^{\mathrm{WN}}_{jj_s}$ and $r^{\mathrm{WN}}_{jj'}$ obey the following equations

$$\begin{aligned}
&\sum_{j'=1}^{N}(A_{jj'} + \delta_{jj'}\sin k_j)r^{\mathrm{WN}}_{j'j_1} = \delta_{jj_1}\sin k_j - A_{jj_1} \\
&\sum_{j'=1}^{N}(A_{jj'} + \delta_{jj'}\sin k_j)t^{\mathrm{WN}}_{j'j_s} = 2\sin k_{j_s}\nu_{j_s j}
\end{aligned} \tag{B3}$$

where the values of the complex wave vector $k_{j(j_s)}$

$$k_{j(j_s)} = k'_{j(j_s)} + \mathrm{i}k''_{j(j_s)} = \begin{cases} k'_{j(j_s)} = 0 & k''_{j(j_s)} > 0 & E_{\mathrm{F}} \in [0, E^{\circ}_j] \\ 0 \leqslant k'_{j(j_s)} \leqslant \pi & k''_{j(j_s)} = 0 & E_{\mathrm{F}} \in [E^{\circ}_j, E^{\mathrm{cl}}_j] \\ k'_{j(j_s)} = \pi & k''_{j(j_s)} > 0 & E_{\mathrm{F}} \in [E^{\mathrm{cl}}_j, 4] \end{cases} \tag{B4}$$

are determined by the energy conservation law $E/2L = \cos k_j + \cos[\pi j/(N+1)] = \cos k_{j_s} + \cos[\pi j_s/(\mathcal{N}+1)]$.

In equation (B4), $E_{\mathrm{F}} = 2 - E/2L$ ($E_{\mathrm{F}} \in [0, 4]$), and the notation $E^{\circ}_j = 1 - \cos(ak_{\mathrm{th}}j)$ ($E^{\mathrm{cl}}_j = 3 - \cos(ak_{\mathrm{th}}j)$) denotes the energy of the opening (closing) of the jth-mode in units $2L$. In the continuum limit, the set (B3) coincides with that used by Szafer and Stone [5].

In the diagonal approximation ($A_{jj'} = \delta_{jj'} A_{jj}$), we have from (B3)

$$\hat{r}^{\mathrm{WN}}_{jj'} \equiv |\hat{r}^{\mathrm{WN}}_{jj'}| \exp(\mathrm{i}\varphi_j) = \delta_{jj'} \frac{\sin k_j - A_{jj}}{\sin k_j + A_{jj}} \qquad \hat{t}^{\mathrm{WN}}_{jj_s} = 2\frac{\sqrt{\sin k_j \sin k_{j_s}}}{\sin k_j + A_{jj}} v_{j_s j}. \tag{B5}$$

Using these expressions in (B2), one finds (also in DA)

$$T^j_{\mathrm{WNW}} = \begin{cases} \left|T^j_{\mathrm{WN}}\right|^2 \Big/ \left[\left|T^j_{\mathrm{WN}}\right|^2 + 4R^j_{\mathrm{WN}} \sin^2(k_j(N_1 - 1) + \varphi_j)\right] & E_{\mathrm{F}} \in [E^{\mathrm{o}}_j, E^{\mathrm{cl}}_j] \\ \left|T^j_{\mathrm{WN}}\right|^2 \Big/ \left[\left(\exp(k_j(N_1 - 1)) + R^j_{\mathrm{WN}} \exp(-k_j(N_1 - 1))\right)^2 + 4R^j_{\mathrm{WN}} \sin^2 \varphi_j\right] & \\ \qquad E_{\mathrm{F}} \in [0, E^{\mathrm{o}}_j] \text{ or } [E^{\mathrm{cl}}_j, 4] & \end{cases} \tag{B6}$$

where φ_j is defined in (B5), and

$$T^j_{\mathrm{WN}} = \sum_{j_w=1}^{\bar{j}_w} |\hat{t}^{\mathrm{WN}}_{jj_w}|^2 = \frac{4|\sin k_j| \Re(A_{jj})}{|A_{jj} + \sin k_j|^2} \qquad R^j_{\mathrm{WN}} = |\hat{r}^{\mathrm{WN}}_{jj}|^2 = \left|\frac{A_{jj} - \sin k_j}{A_{jj} + \sin k_j}\right|^2. \tag{B7}$$

The quantities which enter the expression for the partial transmission T^j_{WNW} are the jth-mode transmission ($|T^j_{\mathrm{WN}}|$) and reflection (R^j_{WN}) probabilities, and the phase of the reflection amplitude (φ_j) in the WN structure. (The term 'probability' is appropriate only for energies $E_{\mathrm{F}} \in [E^{\mathrm{o}}_j, E^{\mathrm{cl}}_j]$. Outside the jth-subband energy interval, the quantities $|T^j_{\mathrm{WN}}|$, R^j_{WN}, and φ_j do not have a particular physical meaning.) Note that taking into account equation (B4) and the symmetry properties of matrix **A**, see (A3), it is easy to prove that

$$\begin{aligned} &|T^j_{\mathrm{WN}}(E < 0)| = |T^{N+1-j}_{\mathrm{WN}}(|E|)| \qquad R^j_{\mathrm{WN}}(E < 0) = R^{N+1-j}_{\mathrm{WN}}(|E|) \\ &\varphi_j(E < 0) = -\varphi_{N+1-j}(|E|). \end{aligned} \tag{B8}$$

The latter relations significantly reduce the number of calculations.

It is easy to verify that equation (B1) with T^j_{WNW} defined in (B6) is just another form of expression (7).

In the continuum limit, the transmission coefficient found in the diagonal approximation takes the form

$$T^{0\mathrm{c}}_{\mathrm{WNW}}(\varepsilon_{\mathrm{F}}) = \sum_{j=1}^{\infty} T^{0\mathrm{c}\,j}_{\mathrm{WNW}} = \sum_{j=1}^{\infty} \frac{(T^{\mathrm{c}j}_{\mathrm{WN}})^2}{(T^{\mathrm{c}j}_{\mathrm{WN}})^2 + 4R^{\mathrm{c}j}_{\mathrm{NW}} \sin^2(\pi q_j l/w + \phi^{\mathrm{c}}_j)} \tag{B9}$$

where

$$T^{\mathrm{c}j}_{\mathrm{WN}} = \frac{4q_j \Re(A^{\mathrm{c}}_{jj})}{\left|A^{\mathrm{c}}_{jj} + q_j\right|^2} \qquad R^{\mathrm{c}j}_{\mathrm{NW}} = \left|\frac{A^{\mathrm{c}}_{jj} - q_j}{A^{\mathrm{c}}_{jj} + q_j}\right|^2 \qquad \tan\phi^{\mathrm{c}}_j = \frac{2q_j \Im(A^{\mathrm{c}}_{jj})}{|A^{\mathrm{c}}_{jj}|^2 - q_j^2} \tag{B10}$$

and real and imaginary parts of A^{c}_{jj} are defined in (A4).

Let us briefly discuss the characteristics of the WN structure appearing in (B6) and also of the total WN transmission, $T_{\mathrm{WN}} = \sum_{j=1}^{\bar{j}} T^j_{\mathrm{WN}}$. For this, it is helpful to write separately

the definitions of $|T^j_{WN}|$, R^j_{WN}, and φ_j for imaginary and real values of k_j. Precisely,

$$|T^j_{WN}| = \frac{4\sinh k_j'' \,\Re(A_{jj})}{|A_{jj} + i\sinh k_j''|^2} \qquad R^j_{WN} = \frac{\Re^2(A_{jj}) + \left(\Im(A_{jj}) - \sinh k_j''\right)^2}{|A_{jj} + i\sinh k_j''|^2}$$
$$\tan\varphi_j = \frac{2\sinh k_j'' \,\Re(A_{jj})}{|A_{jj}|^2 - \sinh^2 k_j''} \qquad \sinh k_j'' = \sqrt{(E_F + \cos(ak_{th}j) - 2)^2 - 1} \tag{B11a}$$

for $E_F \in [0, E_j^o]$, and for $E_F \in [E_j^o, 2]$

$$|T^j_{WN}| = \frac{4\sin k_j' \,\Re(A_{jj})}{|A_{jj} + \sin k_j'|^2} \qquad R^j_{WN} = \frac{\left(\Re(A_{jj}) - \sin k_j'\right)^2 + \Im^2(A_{jj})}{|A_{jj} + \sin k_j'|^2}$$
$$\tan\varphi_j = \frac{2\sin k_j' \,\Im(A_{jj})}{|A_{jj}|^2 - \sin^2 k_j'} \qquad \sin k_j' = \sqrt{1 - (E_F + \cos(ak_{th}j) - 2)^2}. \tag{B11b}$$

As seen from (B11), $|T^j_{WN}| = 0$ at $E_F = 0$, E_j^o, E_j^{cl}, and 4. In the most of the interval $E_F \in [E_j^o, E_j^{cl}]$, where $T^j_{WN} + R^j_{WN} = 1$, this function is very close to unity. The latter equality does not hold outside the jth subband, i.e. for $E_F \in [0, E_j^o]$ and $E_F \in [E_j^{cl}, 4]$. In these energy intervals, T^j_{WN} is a non-monotonic function with the maxima below (and close to) E_j^o and, similarly, above E_j^{cl}. The function R^j_{WN} monotonically decreases from the value of unity, when the energy moves from E_j^o (E_j^{cl}) towards zero (four).

From the character of the $|T^j_{WN}|$ dependences it follows that the total WN transmission as a function of energy has the form of a staircase with slightly rounded steps. Analytically, this dependence is well described by (j is arbitrary)

$$T_{WN}(E_F \in [E_j^o E_{j+1}^o]) = j - 1 + T^j_{WN}. \tag{B12}$$

It is noteworthy that first, the maximum of $T^j_{WN}(E_F \in [E_j^o E_{j+1}^o])$ deviates very little from unity, and second, this deviation is not changed significantly with the plateau number j in the dependence $T_{WN}(E_F)$.

Thus, the transmission quantization in a WN structure is nearly as perfect as the conductance quantization in an ideal infinite wire. The perturbation of the quantization effect in the WN structure is due to the reflection of electron waves at the wide–narrow discontinuity. In the WNW configuration, two new effects come into play: through channel (constriction) tunnelling, and interference of electron waves reflected from the channel edges. The role of these effects in determining the through channel transmission is discussed in section 4.

References

[1] van Wees B J, van Houten H, Beenakker C W J, Williamson J G, Kouwenhoven L P, van der Marel D and Foxon C T 1988 *Phys. Rev. Lett.* **60** 848

[2] Wharam D A, Thornton T J, Newbury R, Pepper M, Ajmed H, Frost J E F, Hasho D G, Peacock D C, Ritchie D A and Jones G A C 1988 *J. Phys. C: Solid State Phys.* **21** L209

[3] Levinson I V 1988 *Pis. Zh. Eksp. Teor. Fiz.* **48** 273 (Engl. Transl. 1988 *JETP Lett.* **48** 301); 1989 *Zh. Eksp. Teor. Fiz.* **95** 2175 (Engl. Transl. 1989 *Sov. Phys.–JETP* **68** 1257)

[4] Kirczenow G 1988 *Solid State Commun.* **68** 715; 1989 *Phys. Rev.* B **39** 10452

[5] Szafer A and Stone A D 1989 *Phys. Rev. Lett.* **62** 300

[6] Glazman L I and Khaetskii A V 1989 *Europhys. Lett.* **9** 263

[7] Lent G S, Sivaprakasam S and Kirkner D J 1989 *Solid State Electron.* **32** 1137

[8] Castaño E and Kirczenow G 1989 *Solid State Commun.* **70** 801; 1990 *Phys. Rev.* B **41** 3874
[9] Patel N K, Martin-Moreno L, Pepper M, Newbury R, Frost J E F, Ritchie D A, Jones G A C, Janssen J T M B, Singleton J and Perenboom J A A J 1990 *J. Phys.: Condens. Matter* **2** 7247
[10] Castaño E, Kirczenow G and Ulloa S E 1990 *Phys. Rev.* B **42** 3753
[11] Cahay M, Bandyopadhyay S and Frohne H R 1990 *J. Vac. Sci. Technol.* B **45** 1399
[12] Patel N K, Nicholls J T, Martin-Moreno L, Pepper M, Newbury R, Frost J E F, Ritchie D A and Jones G A C 1991 *Phys. Rev.* B **44** 13549
[13] Tekman E and Ciraci S 1991 *Phys. Rev.* B **43** 7145
[14] Chaudhuri S, Bandyopadhyay S and Cahay M 1992 *Phys. Rev.* B **45** 11126
[15] Martin-Moreno L, Nicholls J T, Patel N K and Pepper M 1992 *J. Phys.: Condens. Matter* **4** 1323
[16] Chaudhuri S, Bandyopadhyay S and Cahay M 1993 *Proc. Int. Workshop on Computing and Electronics (Urbana, IL, 1992)* p 305
[17] Ji Zhen-Li 1993 *Semicond. Sci. Technol.* **8** 1561
[18] Xu Hongqi 1993 *Phys. Rev.* B **47** 15630
[19] Leng M and Lent G S 1993 *Phys. Rev. Lett.* **71** 137
[20] Leemput L E C and van Kempen H 1992 *Rep. Prog. Phys.* **55** 1165
[21] Todorov T N and Briggs G A D 1994 *J. Phys.: Condens. Matter* **6** 2559
[22] Klimenko Yu A, Malysheva L I and Onipko A I 1993 *J. Phys.: Condens. Matter* **5** 5215; 1993 *Ukr. Fiz. Zh.* **38** 1358
[23] Onipko A I and Zozulenko I V 1993 *Semicond. Sci. Technol.* **8** 2115
[24] Skjånes J, Hauge E H and Schön G 1995 *Phys. Rev.* B at press
[25] Maaø F A, Zozulenko I V and Hauge E H 1995 *Phys. Rev.* B at press
[26] Landauer R 1957 *IBM J. Res. Dev.* **1** 223; 1970 *Phil. Mag.* **21** 683
[27] Stone A D and Szafer A 1988 *IBM J. Res. Dev.* **32** 384
[28] Büttiker M 1988 *IBM J. Res. Dev.* **32** 317; 1990 *Electronic Properties of Multilayers and Low-Dimensional Semiconductor Structures* ed J M Chamberlain *et al* (New York: Plenum) p 51
[29] Beenakker C W and van Houten H 1991 *Advances in Research and Applications* vol 44, ed H Ehrenreich and D Turnbull (New York: Academic) p 1
[30] Klimenko Yu A and Onipko A I 1994 *Fiz. Nizk. Temp.* **20** N9
[31] Patel N K, Martin-Moreno L, Pepper M, Newbury R, Frost J E F, Ritchie D A, Jones G A C, Janssen J T M B, Singleton J and Perenboom J A A J 1990 *J. Phys.: Condens. Matter* **2** 7247